

Development of a synthetically generated earthquake catalogue towards assessment of probabilistic seismic hazard for Tehran

Mohammad R. Zolfaghari

Received: 9 April 2013 / Accepted: 1 November 2014 / Published online: 9 November 2014
© Springer Science+Business Media Dordrecht 2014

Abstract This paper presents the methodology to develop a synthetically simulated earthquake catalogue for northern Iran. The study area covers the northern boundary of Central Iran Plate, which coincides with the Alborz Mountains. A set of areal seismic sources as well as major active faults and their recurrence relationships is modelled to represent the temporal and spatial distribution of potential earthquakes in this region. Probabilistic sampling of events from various spatial and temporal distribution functions, forming sources of uncertainties, is used to generate synthetic events. Areal seismic sources oriented more towards representation of general and background seismicity, derived from statistical and spatial analyses on historical earthquakes. Recurrence relationships as well as potential maximum magnitudes for seismic sources are estimated from records of historical earthquakes and where available from measured and calculated slip rates from recent GPS surveys in this region. The synthetically generated earthquake catalogue provides a realization of potential earthquakes, each characterized with a defined magnitude, location, focal depth, faulting orientation and recurrence frequency. The catalogue is used for assessment of probabilistic seismic hazard, and the results are presented for a test point in the city of Tehran.

Keywords Earthquake catalogue simulation · Monet Carlo simulation · Tehran · Iran · Alborz

1 Introduction

Probabilistic seismic hazard assessment represents distribution of future seismic ground motions in size, time and space. Probabilistic representation of seismic hazard in this way provides the basis for a range of pre- and post-catastrophe planning tools used by many disciplines such as seismic code development, land and town planning and emergency and

M. R. Zolfaghari (✉)

Civil Engineering Department, K. N. Toosi University of Technology, Tehran, Iran
e-mail: mzolfaghari@catrisks.com

post-earthquake response measures. PSHA methodology facilitates convolution of uncertainties associated with earthquakes distribution in time and space as well as those related to ground motion variability. Probabilistic ground motions with defined probabilities of exceedance within certain period are usually derived from PSHA study, which is well suited as design parameter in earthquake engineering. For certain applications of PSHA such as seismic loss estimation and multi-hazard damage evaluation, the user may require access to sources of probabilistic earthquakes with defined locations and frequencies. This is in particular the case for applications in which other sources of uncertainties need to be taken into account and where there are areas of concerns for correlation effects. In such cases, probabilistic algorithm used in PSHA methodology could be used in order to simulate a synthetically generated earthquake catalogue representing the long-term seismotectonic characteristics of a given region. In this study, the methodology applied to generate such catalogue for an area in northern Iran is presented. Tehran, the capital and most populated city of Iran, with rapidly growing population, is located in this area that is coincided along southern foothills of the Alborz Mountain range and bounded by several active faults. Earthquake hazard in Iran is a serious threat to society and human life in addition to widespread built environment.

There have been several studies in recent years on the earthquake hazard in Tehran and surrounding areas. Nowroozi (2010) used a historical earthquake catalogue within a radius of 300 km around Tehran in order to estimate probabilistic horizontal and vertical PGA for Tehran. His assessment was based on the assignment of maximum magnitude to some of the active faults with no seismogenic source regionalization. Yazdani et al. (2012) used a Monte Carlo simulation process to generate seismic hazard maps on the bedrock in greater Tehran region, resulting in probabilistic PGA of 0.34–0.47 g for 475-year return period. In another study by Ghodrati Amiri et al. (2007) for Tehran, PGAs of 0.27–0.46 and 0.33–0.55 g were estimated for return periods of 475 and 975, respectively. Yaghmaei-Sabegh and Lam (2010) applied a stochastic simulation process to generate accelerograms for a range of earthquakes with magnitude of 6.3–7.4. In a similar study by Zafarani et al. (2009), a stochastic simulation approach was used to simulate strong ground motions records for metropolitan city of Tehran, using characteristics of three active faults in the Alborz range.

These studies, however, lack proper regionalization of seismotectonic environment of the potential seismic sources in the vicinity of Tehran. Besides, they did not properly incorporate sources of uncertainties associated with temporal and spatial distributions of seismicity, upon which a real probabilistic seismic hazard assessment could be based. The present study uses the available seismotectonic information to develop a seismotectonic source model for the city of Tehran and its surrounding. Following in this article, the general seismotectonic setting of the study area is reviewed first. Historical earthquake catalogue and characteristic of major tectonic features are used to define seismogenic source models for the study area. The paper also presents the methodology for assessing frequency–magnitude relationship for characteristics earthquakes on active faults. The methodology used to simulate synthetic earthquake catalogue and various representation of simulated catalogue and verifications against regional seismotectonic characteristics are also presented in this paper.

2 Regional seismotectonic setting

The study area covers an area of some 600 by 800 square kilometres in northern Iran as shown in Fig. 1. Seismicity in the study area is mostly controlled by tectonic deformation

on a few distinct regions. The active belt of seismicity in northern Iran, bordering the South Caspian Basin from Central Iranian Plate, coincides with the Alborz Mountains. The South Caspian Basin is an aseismic block in the Alpine belt, which is surrounded by several zones of high seismic activity (e.g. Berberian 1983). This block is surrounded by the Talesh and Alborz Mountains to the west and south, respectively, and joins the west Turkmenian lowlands at its eastern boundary (Fig. 1). The Talesh and Alborz Mountains are overthrusting the “oceanic-like crust” of the South Caspian Basin (e.g. Berberian 1983). Recent GPS survey indicates roughly northward motion of South Caspian Basin at 6.5 ± 2 mm/year relative to Eurasia (Vernant et al. 2004). The Central Iran Plate is bordered by the Zagros Folded belt in the south-west, the Alborz Mountains in the north and the Lut Block in the east (Fig. 1). It is generally accepted that the Central Iran Plate appears to be much less active than the regions surrounding them (e.g. Berberian and Yeats 2001).

Main tectonic features posing seismic hazard to the city of Tehran are controlled by deformation along the Alborz Mountain range. This range is an active EW trending belt of some 100 km wide and 600 km long. It is bounded by the Talesh Mountains to the west and the Kopet Dagh Mountains to the east (e.g. Berberian 1983; Alavi 1996). A total shortening of some 30 km since the early Pliocene is estimated across this belt at the longitude of Tehran (Allen et al. 2003). North–south shortening and sinistral shearing across the Alborz are estimated 5 ± 2 mm/year and 4 ± 2 mm/year, respectively, according to GPS data (Vernant et al. 2004). Several active faults, mostly parallel to the range and forming V-shaped pattern, accommodate the present-day oblique convergence across the mountain belt (e.g. Berberian and Yeats 2001; Allen et al. 2003; Ritz et al. 2006). Present-day deformation in Alborz is characterized by the range parallel left-lateral strike-slip and thrust faults as supported by the CMT solutions from recent events (Jackson et al. 2002).

The recurrence of moderate to large earthquakes in the Alborz suggests significant deformation of this mountain belt. This belt has been responsible for many catastrophic historical earthquakes (Tchalenko 1975; Ambraseys and Melville 1982, Berberian and Yeats 2001), also supported by instrumental seismicity (Ambraseys and Melville 1982; Engdahl et al. 2006). The Manjil earthquake of 20 June 1990, which is the most disastrous Iranian earthquake in the twentieth century, occurred in this belt. The main seismotectonic sources posing near-field seismic hazard to the city of Tehran are located in this belt as well as some moderate active faults in the northern part of Central Iran Plate (Fig. 1).

3 Past seismicity

An earthquake catalogue is compiled for the study area consisting of pre-1900 historical events as well as post-1900 macroseismic and instrumental events. A working catalogue is prepared for this region based on the available information from various sources. The pre-1900 historical part consists of mainly data prepared by Ambraseys and Melville (1982), which refers to earthquakes as old as 400 BC and contains references to 256 pre-1900 historical earthquakes for Iran. For post-1900 events, epicentral locations recalculated by Ambraseys and Melville (1996), ISC catalogue and Harvard estimates after 1980 have been used. The database lacks homogeneity and completeness in time and space and therefore needs further process to examine completeness and to make a uniform magnitude scale. Figure 2 illustrates the geographical distribution of moderate to large earthquakes up to 2010 for this region. A majority of small to moderate magnitude events in the working catalogue are dependent shocks, mostly recorded in the last few decades. The de-clustering

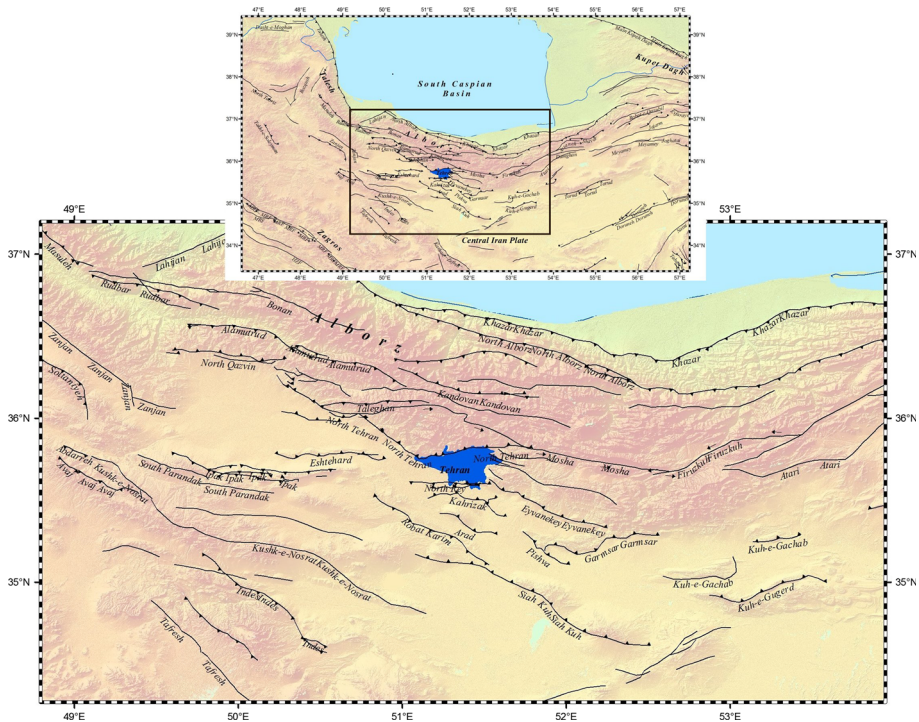


Fig. 1 Major plate boundaries engaged in seismotectonic of northern Iran, posing seismic hazard to the city of Tehran

algorithm proposed by Gardner and Knopo (1974) is used to remove dependent events from the compiled catalogue. The compiled catalogue for this region refers to some 1,050 independent events with $M_w \geq 4.0$ as shown in Fig. 2.

In general, reliable focal depth estimates are not available for earthquakes prior to 1963 for this region. For post-1963 earthquakes, the focal depths reported by the ISC are used in the seismicity database. Seismicity in Iran is dominated by shallow thrust and strike-slip faulting at depths of less than 50 km. To summaries, the Iranian seismicity can be assumed of shallow depth earthquakes (less than 30 km) except for the occasional and unverified shocks at southern part of Zagros and Makran regions.

4 Areal seismic source model

A seismotectonic source model represents distribution of future earthquakes in space, time and size. For regions with seismic activity generated by diffused patterns of small to moderate faults, earthquake sources are modelled by area source zones that are usually defined based on a combination of historical seismicity and characteristics of tectonic features. In this paper, the seismogenic sources are modelled by area sources, based on the relationship between clustering of short-term seismic activity and the regional long-term tectonic movements as well as large-scale faulting activities. Figure 3 shows the delineated boundaries for these seismic sources in conjunction with past seismicity and major tectonic

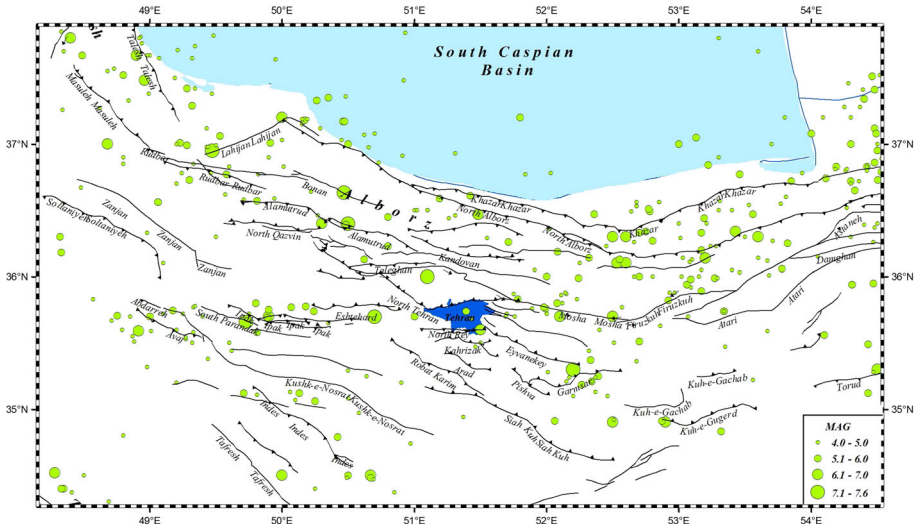


Fig. 2 Geographical distribution of moderate to large earthquakes up to 2010 including historical earthquakes for the study area with $M_w \geq 4.0$

features. In addition to the epicentral maps usually used in defining source zones, other maps representing spatial and temporal distribution of seismicity such as smoothed earthquake frequency and smoothed cumulative seismic moment maps are used here. Figure 4 shows boundaries of proposed seismic source zones against smoothed frequency of earthquakes with magnitude $M_w \geq 4.0$. Similar map is shown in Fig. 5, illustrating source boundaries against smoothed seismic moment released over the last 1,200 years. The delineated seismic sources are used to test the completeness of seismicity data and to construct the frequency–magnitude relationships as well as estimation of maximum magnitude for each source. Historical and instrumental earthquake catalogue is the main source of information for regionalization and parameterization of seismogenic source zones. The compiled earthquake catalogue described earlier is used for this process.

Geographical as well as temporal incompleteness usually results in inhomogeneous earthquake catalogues. The incomplete seismicity database needs to be treated before it can be used for seismic hazard analysis. In this study, the statistical method proposed by Stepp (1972) is used for earthquake catalogue completeness test. This method helps to estimate time subintervals for which particular magnitude class is likely to be completely reported. The Stepp’s statistical test was carried out for seismicity in all seismic sources, and estimated time subintervals are used in order to calculate frequency–magnitude relationships described in the next section. Figure 6 shows the results of completeness investigations for one of the seismic sources in this study. The time interval for which each magnitude class is completely reported can be estimated from such figures. The present catalogue as a whole seems to be reasonably complete for earthquakes with magnitudes $M_w > 4.4$ back to around 1960 and for $M_w > 5.2$ back to 1900. The completeness time tends to be longer for higher magnitude intervals.

The seismicity parameters are estimated, incorporating completeness criteria for various magnitude intervals. In this paper, two types of recurrence relationships are used in order to define seismotectonic characteristics for each seismic source. Exponential recurrence

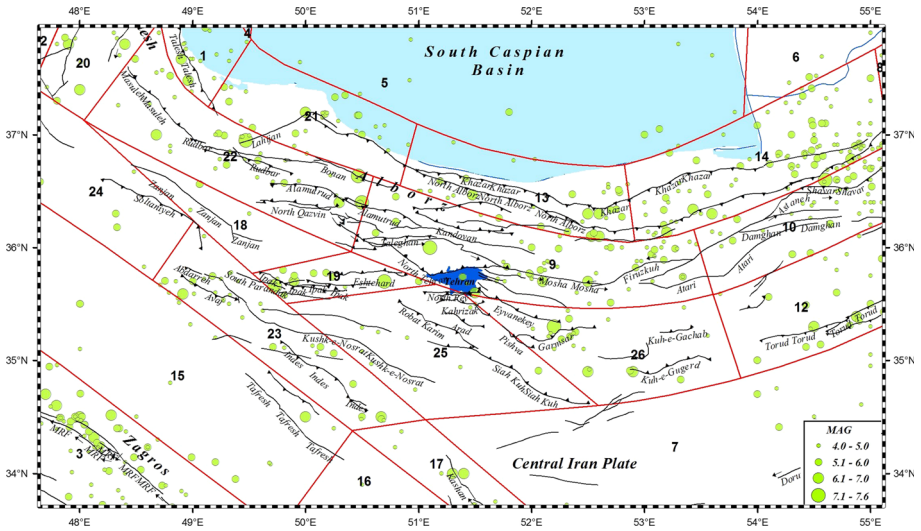


Fig. 3 Seismic source model for the study area, showing boundaries of proposed seismic source zones against past seismicity and major tectonic features

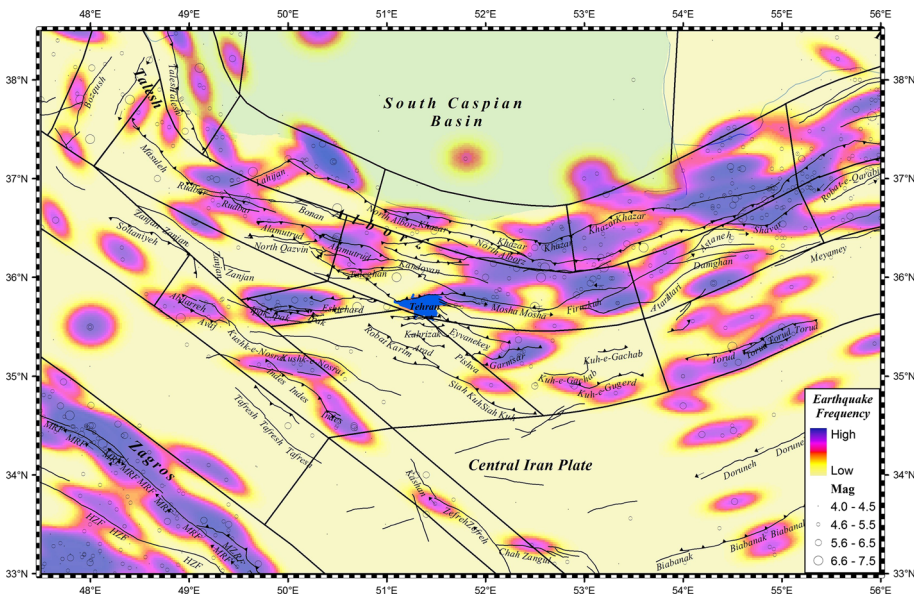


Fig. 4 Geographical distribution of smoothed seismicity (frequency) of earthquakes with $5 \leq M_w < 6.0$ against boundaries of proposed seismic sources

relationship, known as Gutenberg–Richter relationship, is used to model recurrence rates of small to moderate seismicity ($4.0 \leq \text{magnitude} < 6.5$) and for seismic sources with diffused seismicity and no apparent influences of individual fault. However, for sources dominated by individual fault, combined exponential–characteristic model is used, which

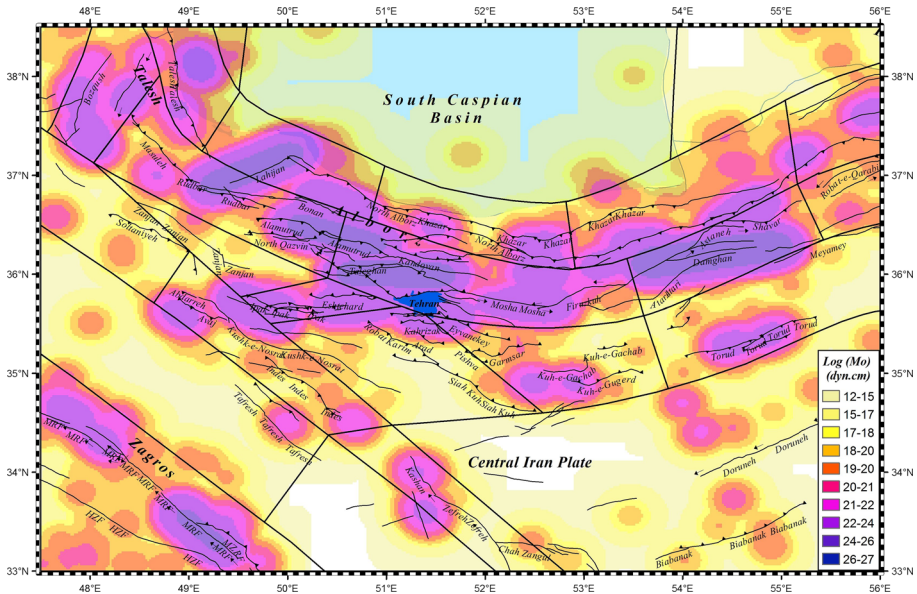


Fig. 5 Seismic source boundaries against smoothed annual seismic moment released for the last 1,200 years

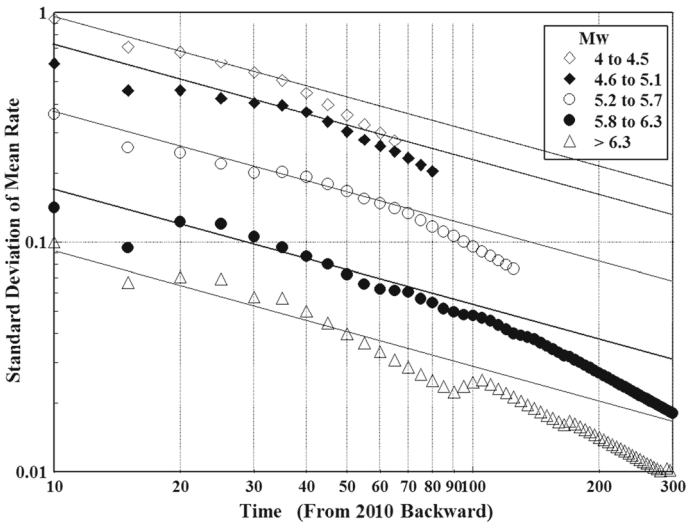


Fig. 6 Results of completeness test (Stepp Method) for one of the seismic sources in the study area

reveals better fitness to historical earthquakes. Equations (1) and (2) show normalized truncated forms of exponential and combined exponential–characteristic relationship, respectively (e.g. Schwartz and Coppersmith 1984).

$$N(M) = N(M_o) \frac{e^{-\beta(M-M_o)} - e^{-\beta(M_{\max}-M_o)}}{1 - e^{-\beta(M_{\max}-M_o)}} \quad M_o \leq M \leq M_{\max} \tag{1}$$

$$N(M) = \begin{cases} N_e \frac{e^{-\beta(M-M_o)} - e^{-\beta(M_{\max}-M_o)}}{1 - e^{-\beta(M_{\max}-\Delta M-M_o)}} & M_o \leq M < M_c \\ N_c \frac{M_{\max} - M}{\Delta M} & M_c \leq M < M_{\max} \end{cases} \tag{2}$$

In which M_o and M_{\max} are minimum and maximum magnitudes, respectively, $N(M_o)$ is the number of earthquakes larger than minimum magnitude (M_o), N_c is the number of earthquakes larger than $M_c = M_{\max} - \Delta M$ and $N_e = N(M_o) - N_c$ is the number of earthquake with magnitude $M_o \leq M < M_c$. Two regression methods, the least square and the maximum likelihood approaches, are used in order to estimate $N(M_o)$ and β in Eqs. (1) and (2). Figure 7 shows examples for these frequency–magnitude relationships. Depending on seismogenic source type and availability and reliability of seismotectonic data, maximum magnitude (M_{\max}) is estimated from historical observations, from tectonic characteristics, or where data are sufficient, from statistical analyses on earthquake data. Table 1 lists the estimated values for Gutenberg–Richter a and b values as well as $N(M \geq 4.0)$ and M_{\max} for the delineated seismic sources in this study.

4.1 Seismic source uncertainties

In most seismic hazard studies, the Gutenberg–Richter parameters are usually assumed to be uniformly distributed over seismically homogeneous area sources. Such normalization of seismicity over a large area makes the calculated seismic hazard too dependent to the shape of delineated seismic source boundaries. In the present study, a hybrid approach proposed by Zolfaghari (2009) is used, in which the boundaries of seismic sources are converted into a grid data layer, providing a cell-based source system. In this method, the future earthquake locations are modelled according to the scattered location of past seismicity, taking into account the regional seismotectonic characteristics estimated for each seismic source. Each cell in the cell-based model represents an individual seismic source, capable of implementing many tectonic- and seismicity-related variables into the hazard estimation process. One of such variation is non-uniformity of activity rates across seismic source, which could be implemented using smoothed seismicity layers.

The smoothing process is an attempt to spread regional seismicity along causative tectonic features and also to take into account the uncertainties associated with the locations of past earthquakes as well as giving some weight to the new locations for future earthquakes. Two alternative smoothing processes as proposed by Zolfaghari (2009) are used here. For small to moderate earthquakes, a symmetric 2D Gaussian distribution (Fig. 8a) is used, while for larger earthquakes, 2D Gaussian distribution with higher standard deviation along fault rupture is used (Fig. 8b). This smoothing process is performed in several grid layers, each representing frequency of events with a given magnitude interval. Examples of such smoothed maps are shown for earthquake frequencies in Fig. 10. In this study, the smoothed earthquake frequency layers are used to weight the Gutenberg–Richter parameters across each seismic source. This is in contrast to the conventional source zone methods in which activity rate is uniformly distributed across seismic source zones. The Gutenberg–Richter a value for each source is weighted based on the normalized smoothed seismicity using Eq. 3 (Zolfaghari 2009):

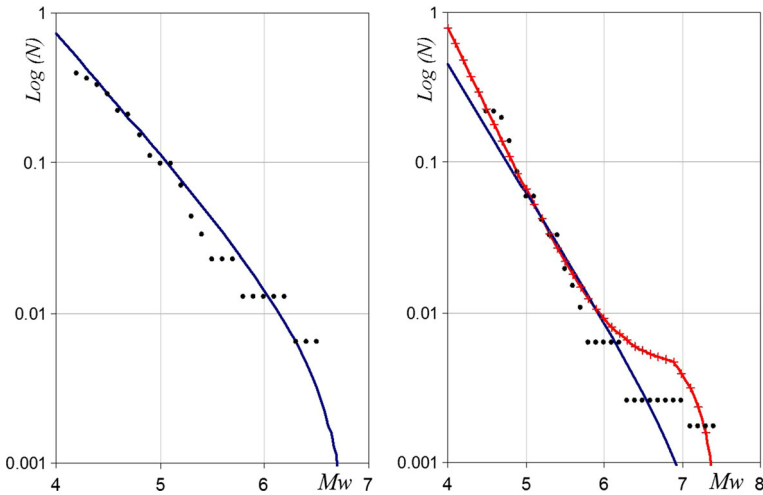


Fig. 7 Frequency–magnitude relationships for major seismic sources in the vicinity of Tehran. The black curve in both graphs shows exponential frequency–magnitude relationships while the red curve in right graph represents characteristic earthquake behaviour at larger magnitude levels

$$\alpha_i = a + \log \omega_i + \log(S_o/s_i) \tag{3}$$

In which a and α_i are Gutenberg–Richter a value for main seismic source and source cell i , respectively, which represent the logarithm of cumulative frequencies of earthquakes with $M \geq 0$ per square kilometre. Also in this equation, $\omega_i = n_i/N_o$ represents weighting factor for each cell, and S_o and s_i represent the seismic source and cell surface area, respectively (Fig. 8c) where $N_o = \sum n_i$ and $S_o = \sum s_i$. For example, for a main source with $a = 1.5$ and $S_o = 2,000 \text{ km}^2$ divided into two cells with $n_1 = 3, s_1 = 500$ and $n_2 = 2, s_2 = 1,500$, the equation results in $\alpha_1 = 1.880$ and $\alpha_2 = 1.227$. Past seismicity can be spatially smoothed for several magnitude intervals rather than in a cumulative sense. In this case, ω_i and α_i represent the frequency and cumulative frequency of events with $M_1 < M \leq M_2$, respectively, and the same formulation can be extend to cover all magnitude intervals.

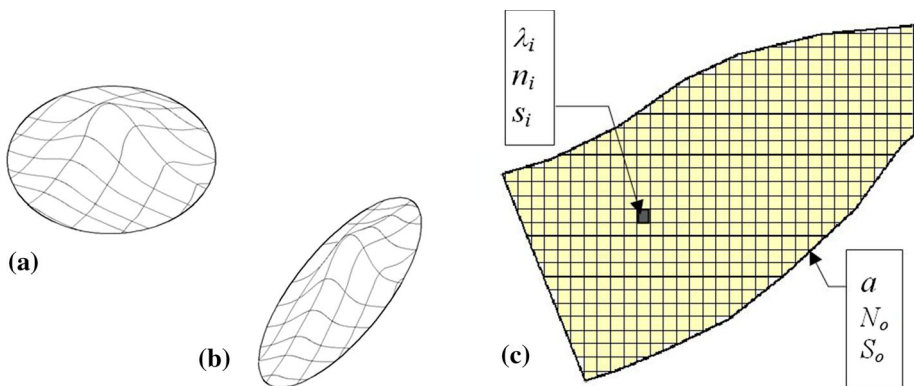
The same approach is used to spread aggregated seismic moment along tectonic features as shown in Fig. 5. The cell-based source model also provides enhancement to many other aspects of the conventional seismic hazard methodology and also provides facilities for implementation of many other seismotectonic factors into the seismic hazard estimation. Using such cell-based algorithm, several grid layers, each representing an aspect of regional seismotectonic characteristics, are modelled and used in this study.

4.2 Modelling fault geometry using cell-based source model

The simplest geometric feature used to model rupture segments in many seismic hazard assessment tools is line segments, each representing the projection of a vertical rupture plane on the surface. Regardless of the simplicity of such model, the fault-to-site distance measurement used in many ground motion prediction equations is achievable using such representation for fault ruptures. Depending on the sizes of earthquakes, fault ruptures can extend over a few to several hundreds of kilometres. In order to enhance fault-to-site distance calculation, the cell-based method is used to implement rupture geometry into the

Table 1 Estimated values for Gutenberg–Richter a and b values as well as $N(M \geq 4.0)$ and M_{\max} for the delineated seismic sources

Source	a value (G–R)	b value (G–R)	$N(M \geq 4.0)$ per year	M_{\max}
1	3.17	0.84	0.561	6.9
2	3.46	1.00	0.120	6.8
3	4.64	1.10	6.927	7.3
4	3.46	0.98	0.055	6.2
5	2.99	1.00	0.765	6.0
6	3.47	1.00	0.606	6.0
7	3.07	1.03	0.912	6.3
8	4.52	1.10	1.343	7.5
9	4.30	1.10	1.788	7.3
10	4.40	1.10	1.399	7.4
11	4.54	1.10	0.848	7.0
12	2.58	0.86	0.278	6.3
13	4.50	1.10	1.877	7.0
14	4.22	1.02	3.251	7.0
15	2.67	0.96	0.299	6.0
16	2.61	1.01	0.074	6.0
17	2.90	1.00	0.099	6.7
18	2.71	0.83	1.050	7.0
19	4.30	1.10	1.423	7.3
20	3.50	1.00	0.352	7.2
21	3.63	0.97	0.768	6.4
22	4.30	1.10	1.641	7.6
23	3.07	0.80	1.193	6.8
24	2.95	0.90	0.347	6.1

**Fig. 8** Application of normal distribution function to smooth the observed seismicity based on: **a** Point source model, **b** 2D distribution with larger scatter along fault rupture, **c** Use of spatial distribution of historical seismicity to weight seismic activity rate (a value) (Zolfaghari 2009)

hazard assessment framework. As explained earlier, the line segment provides the simplest representation of fault rupture in order to model faulting effect in seismic hazard models. In practice, the location and length of fault segments are derived from fault lines shown on fault maps or other detailed seismotectonic studies. The approach used in this paper is based on the generalization of available seismotectonic information, presented in the form of simple line segment map. Each line in this map represents a specific fault or fault zone. To construct such line segment map, a combination of the following information is used:

- Faulting orientation derived from tectonic and Quaternary active fault maps
- Tectonic slip vector in conjunction with other geographical features such as topography and mountain ranges
- Shaking intensity contour maps derived from filed observations and reported from historical earthquakes
- Fault plane solutions for events larger than $M_w > 5.5$, providing information about fault mechanisms as well as rupture orientation

Line segments, showing the orientation of potential fault ruptures, are drawn as shown in Fig. 9. The attribute information linked to each line segment is further distributed into a wider region in the vicinity of each line segment using GIS spatial buffer analyses. The conversion of these buffer zones into cell-based system allows transferring fault-related data to the seismic hazard assessment tool (Fig. 9). The attribute information assign to each line segment in this system could vary from simply fault azimuth and dip angles to several other geometric measures representing full 3D rupture plane (Fig. 9a). In the present study, the attribute data include faulting azimuth, ranging from 0 to 360 degree, and the coordinates of endpoints for each line segment. Rupture lengths are estimated from empirical relationships relating rupture length to earthquake magnitude. For this purpose, the following empirical relationship proposed by Ambraseys and Melville (1982) is used.

$$\log L = 0.7M - 3.24 \quad (4)$$

In this relationship, L is rupture length in km and M refers to surface wave magnitude. Probabilistic earthquakes generated in each seismic source are assigned line ruptures based on the fault attribute data derived from cell-based system. A bilateral rupturing pattern is assumed for each probabilistic earthquake in order to calculate source-to-site distances. Epicentral distance (Fig. 9b) and the closest distance to the surface projection of fault rupture (Fig. 9c) can be estimated using this algorithm (Zolfaghari 1998, 2009). These distance definitions are the most common source-to-site distances used in many ground motion prediction equations.

5 Simulation approach

PSHA methodology provides exceedance probability for various levels of ground motions by combining several sources of uncertainties. The approach proposed by Cornell (1968) forms algorithm for main analytical tools used for such assessment. The results provided by such tools fit well for engineering purposes and many other applications. However, there are other applications of PSHA in which access to the underlying probabilistic earthquakes is required. Hazard disaggregation procedure (e.g. Mc Guire 1995) attempts in providing pairs of earthquake magnitude and distance, which have main contribution to the design ground motion. In probabilistic seismic loss assessment used by decision-makers

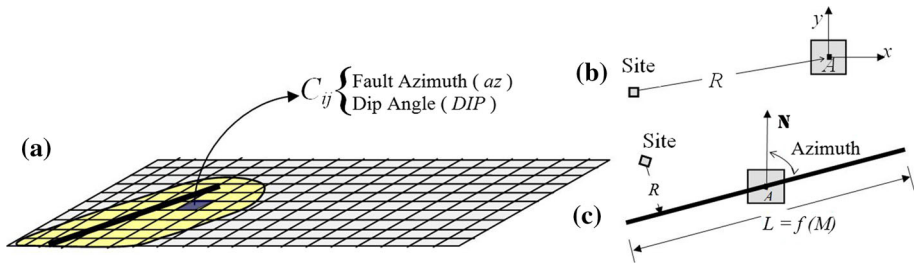


Fig. 9 Cell-based source system; **a** fault attribute data modelled for each cell. **b** Epicentral distance, **c** closest distance to fault line (Zolfaghari 1998, 2009)

and insurance industry and in cases where multi-seismic hazard and damages need to be assessed, it is essential to have access to every single events contributing to the overall probability of exceedance. In this paper, Monte Carlo simulation approach is used to develop synthetically generated probabilistic earthquake catalogue. The approach is based on sampling from various distribution functions representing events scattering in time, space and other tectonic characteristics.

6 Monte Carlo earthquake catalogue simulation

In this study, Monte Carlo simulation process is used to simulate earthquake catalogue of a given length of time (T). In this approach, the frequency–magnitude relationship (Eqs. 1, 2) for each seismic source is used to generate a list of earthquakes, each with a given magnitude. $N(M)$ in these equations represent the annual cumulative frequency of events with $M_o \leq M < M_{\max}$ in each zone. Simulation of an earthquake catalogue worth of T years results in $n = T \times N(M_o)$ events of $M \geq M_o$. For example, 1,000-year earthquake simulation for a seismic source with $N(M_o) = 0.2$ results in 200 events with magnitude derived from the inversed format of Eq. (1) or 2, i.e. $M = f(N(M_o), \beta, n-j)$, where $j = 1, 2, \dots, 200$ represents the sequence of events being simulated. The first event in this sequence has magnitude of $M = M_o$ and the last one $M < M_{\max}$. Every event simulated in this way needs to be located somewhere in the source zone. The smoothed seismicity map (Fig. 10) is used as a two-dimensional density function in the Monte Carlo simulation process, returning a longitude and latitude for each simulated earthquake. Monte Carlo simulation process uses these density functions for each seismic source in order to choose random location for epicentres, and as a result, simulated earthquake catalogue follows the same geographical pattern as the smoothed seismicity layers. In this study, smoothed seismicity maps for various magnitude intervals (e.g. Fig. 4) are used as spatial distribution density function in order to locate earthquake epicentres for each magnitude interval. The approach used in the study allows the user to mix uniform and non-uniform (smoothed) distribution based on defined weights. Monte Carlo simulation process based on a uniformly distributed source model gives equal chance to each location within the source area, and therefore, simulated catalogue will show uniformly random distribution of earthquake epicentres. In a similar pattern, each simulated earthquake is given a random depth, derived from depth distribution function, in this case a normal distribution with estimated mean and standard deviation for each seismic source.

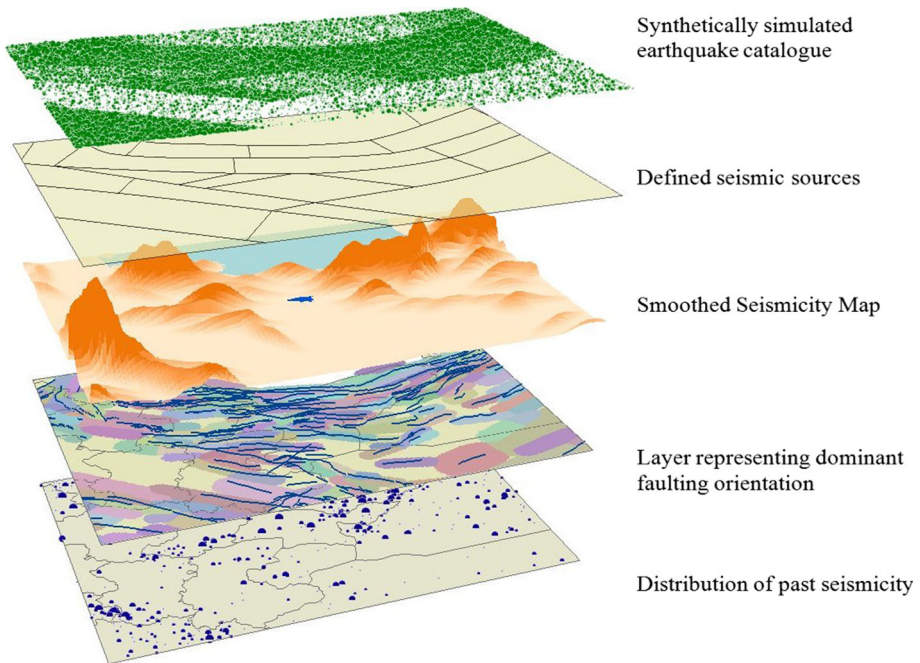


Fig. 10 Application of various geographically distribution layers to represent spatial and temporal distribution of regional seismotectonic characteristics for earthquake simulation process

The cell-based seismic source model described earlier facilitates the assignment of faulting orientation to each simulated earthquake using raster data layer representing faulting orientation. The geographical layer representing faulting azimuth (Fig. 10) returns a faulting azimuth for simulate longitude/latitude. Based on earthquake magnitude and L – M empirical relation such as Eq. (4), a rupture length is also given to each simulated event. Figure 10 illustrates these steps geographically. Following the same approach for all seismic sources in the study area, we can derive a synthetically simulated earthquake catalogue worth of T years. Each simulated earthquake is also given a random year number (between 0 and T) and a random day number (between 1 and 365). Figure 11 illustrates such catalogues for 1,000 years with uniform distribution, with non-uniform distribution and with 30 % uniform and 70 % non-uniform distribution.

7 Results and discussion

The simulation approach used in this study provides a framework for simulating earthquake catalogues of given length of time. Such catalogues could be used in various seismic hazard and risk assessment studies. Figure 12 shows distribution of annual rate of seismic moment from simulated earthquake catalogue. This map could be compared against similar map derived from historical earthquakes (Fig. 5), illustrating consistency of simulated earthquakes, both in terms of geographical pattern as well as rate of seismic moment. The 1,000-year simulated earthquake catalogue (Fig. 11) shows much higher number of small

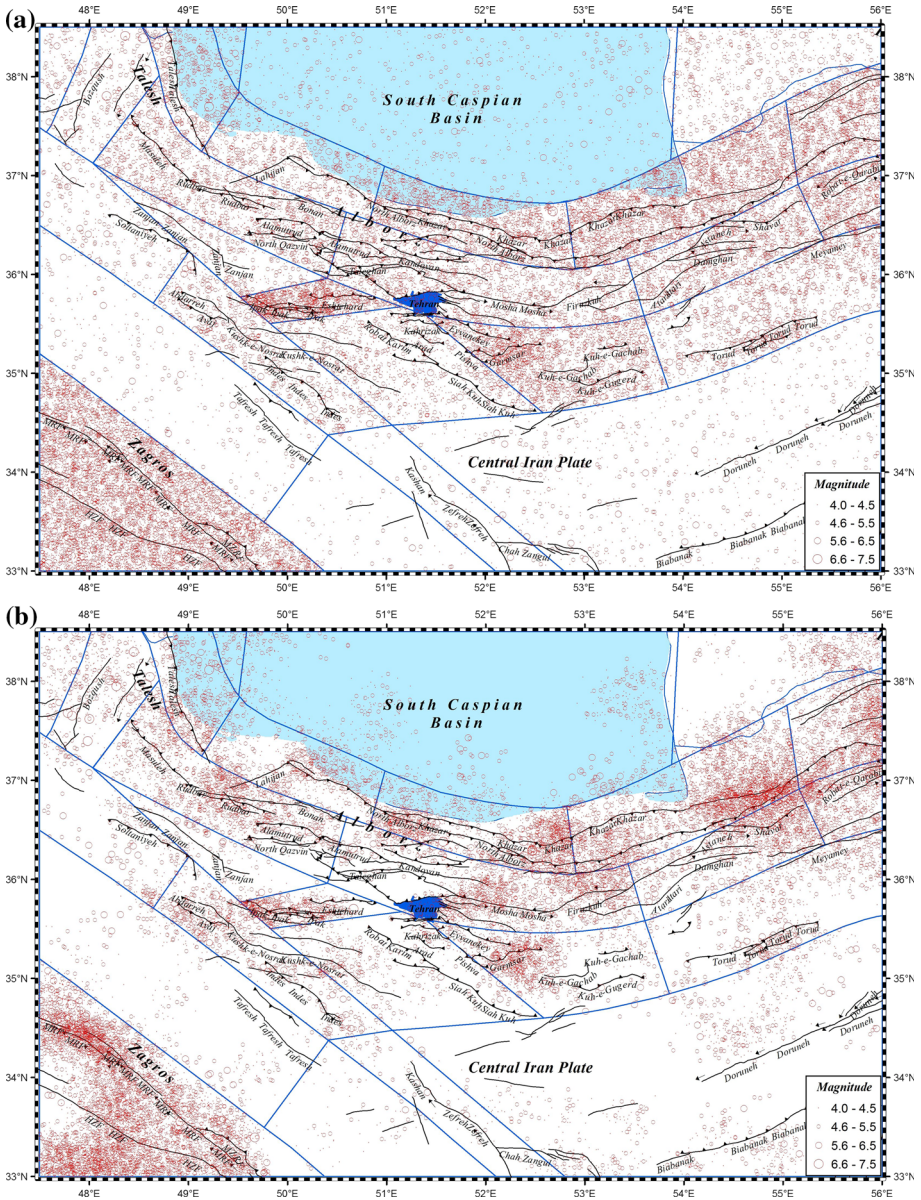


Fig. 11 Synthetically simulated earthquake catalogue for 1,000 years using Monte Carlo simulation process: **a** with uniform spatial distribution, **b** with non-uniform distribution using smoothing pattern, **c** with 30 % uniform and 70 % non-uniform distribution

to moderate earthquakes compared to the historical earthquake catalogue of similar length (Fig. 2). This is due to incompleteness of historical earthquake catalogue for smaller events. The same effect is seen in the seismic moment map generated out of the simulated

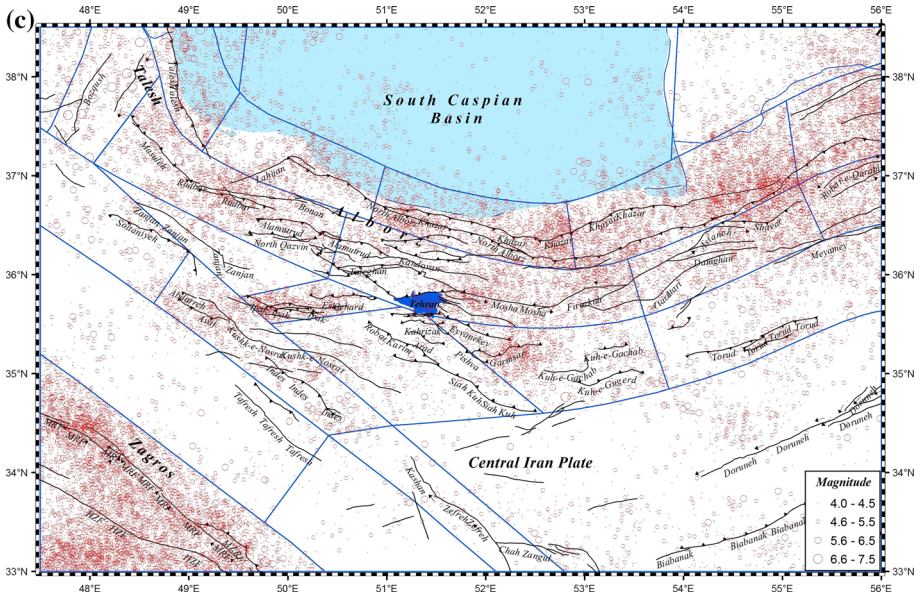


Fig. 11 continued

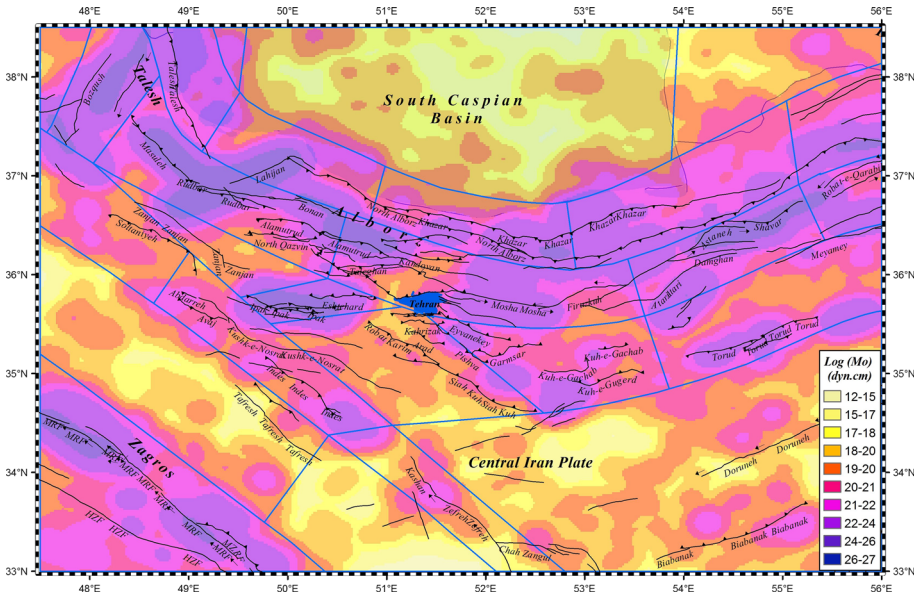


Fig. 12 Annual seismic moment estimated from synthetically simulated earthquake catalogue

earthquakes (Fig. 12) where it is compared against the same map from historical earthquakes (Fig. 5). Simulated earthquake map shows higher background rate of moment released in less active areas.

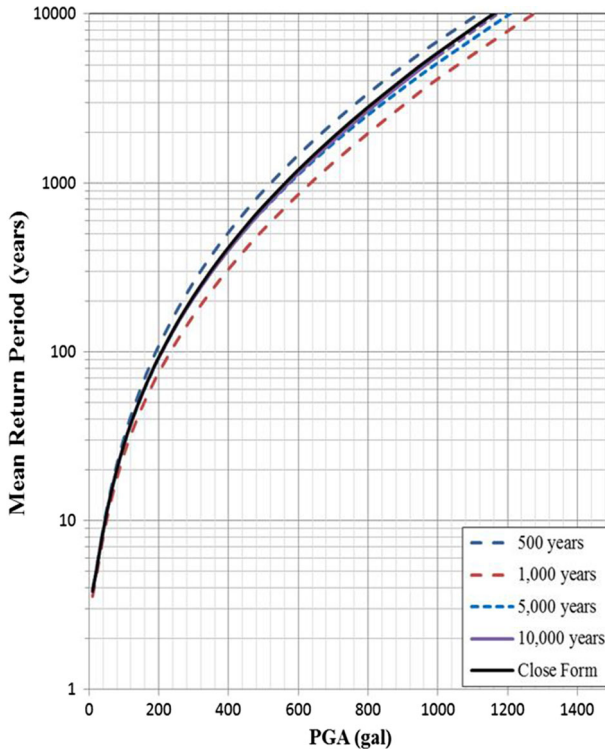


Fig. 13 Comparison of probabilistic PGA derived from synthetically generated earthquake catalogues of various lengths for a site with soft soil condition in Tehran

Like other applications of Monte Carlo process, the number of sampling should be large enough to ensure full coverage of distribution functions representing uncertainties for each component. The length or duration of simulated earthquake catalogue in this study represents the number of time that Monte Carlo simulation process is used to generate earthquake catalogue. To illustrate such sensitivity, probabilistic seismic hazard curves are developed using simulated earthquake catalogue. Simulated catalogues of 500, 1,000, 5,000 and 10,000 years are used to derive hazard curves for a site in the centre of Tehran ($\varphi = 35.72^\circ$, $\lambda = 51.37^\circ$). As a benchmark, hazard curves are also estimated using the closed-form solution, based on Cornell (1968) approach. For this exercise, the ground motion prediction equation proposed by Campbell and Bozorgnia (2008) is used. This equation is parameterized to represent ground motion for soft rock conditions, with NEHRP class B and shear wave velocity of $560 < V_s < 760$ m/s. The cell-based source model used in this article (Zolfaghari 2009) allows assignment of other source-specific information to each simulated earthquake. This information includes faulting azimuth, dip angle, rupture length, rupture width and focal mechanism, which facilitates three-dimensional representation of source geometry and calculation of complex source parameters, such as distance to the top of ruptures, shortest distance to the rupture and focal mechanism and hanging wall location, used in NGA ground motion prediction equations.

Figure 13 shows PGA against annual rate of exceedance for four simulated catalogue as well as the closed-form solution. Hazard curves converge to the closed-form solution as the

length of simulated earthquake catalogue increases. The differences between closed-form solution and the simulated catalogue are higher at the high return periods, which are due to inability of simulated catalogue to include samples of large earthquakes, particularly for catalogues with shorter length of simulation.

Use of Monte Carlo simulation process in estimating probabilistic seismic hazard curves may not present that much improvement to the approach originally proposed by Cornell (1968), as both approaches result in hazard curves similar to those shown in Fig. 13. However, there are applications of probabilistic seismic hazard assessment in which access to each event causing hazard is required or where multi-hazard seismic loss assessment is required. In case of multi-hazard loss estimation, use of Monte Carlo simulation helps better handling of correlation issues. For example, in the process of seismic damage assessment for different component of a lifeline system, estimation of PGA as well as PGV or PGD may be required. Conventional seismic hazard program could provide hazard curves for each of these ground motion agents; however, simultaneous use of these probabilistic curves raises the issue of correlation. Other application is where aggregated effect of seismic hazard over certain period is required. Given that each event in the simulated earthquake catalogue is tagged with a year and day number, annual aggregation of earthquake consequences (e.g. economic losses) is straight forward with no need for further proxy method. This is in particular the main advantage of such simulation process in application of catastrophe modelling in the insurance industry.

8 Conclusion

The conventional PSHA methodology convolutes uncertainties associated from earthquake occurrence and ground motion prediction equations. The results obtained from such analysis are well suited for the engineering applications and design seismic code purposes. However, there are other applications of PSHA in which access to individual simulated earthquake is required. In this article, the methodology and practical example for application of Monte Carlo simulation in the assessment of seismic hazard are presented. This approach allows modelling many earthquake scenarios, representing regional seismotectonic characteristics. The earthquakes simulated in this way are assigned source parameters and date and time, simulating real historical earthquake catalogue but with much longer time span and complete in all magnitude ranges. To illustrate its use and to compare the results with conventional PSHA methodology, a pilot study is performed in this article, using regional seismotectonic characteristics of northern Iran. Various geographical representations of seismotectonic sources and variability associated with location, activity rate, tectonic features, focal depth and seismic moment are used in the development of these sources. Synthetic earthquake catalogues are simulated using Monte Carlo simulation process in conjunction with distribution functions representing epistemic and aleatory uncertainties associated with earthquake sizes and recurrence rates, location and faulting orientation. Each simulated earthquake is characterized with epicentre location, focal depth, rupture length and width, strike and dip angles, focal mechanism and date and time. This information facilitates construction of three-dimensional source geometry and calculation of source-to-site distance definitions used in the NGA ground motion prediction equations. PSHA hazard curves are estimated for a test point in the city of Tehran using the simulated earthquake catalogues as well as numerical calculation of closed-form solution.

Results show high sensitivity of hazard curves to the length of simulated earthquake catalogues, particularly at the high return periods.

References

- Alavi M (1996) Tectonostratigraphic synthesis and structural style of the Alborz mountain system in northern Iran. *Geodynamics* 21(1):1–33
- Allen MB, Ghassemi MR, Sharabi M, Qorashi M (2003) Accommodation of late Cenozoic oblique shortening in the Alborz range, Iran. *J Struct Geol* 25:659–672
- Ambraseys NN, Melville CP (1982) A history of Persian earthquakes. Cambridge University Press, Cambridge 219
- Ambraseys NN, Melville CP (1996) The catalogue of Persian Earthquakes. Internal report. Imperial College of Science and Technology, University of London, UK
- Berberian M (1983) The southern Caspian: a comparison depression floored by a trapped, modified oceanic crust. *Can J Earth Sci* 20:163–183
- Berberian M, Yeats RS (2001) Contribution of archeological data to studies of earthquake history in the Iranian Plateau. *J Struct Geol* 23:563–584
- Campbell KW, Bozorgnia Y (2008) NGA ground motion model for the geometric mean horizontal component of PGA, PGV, PGD and 5% damped linear elastic response spectra for periods ranging from 0.01 to 10s. *Earthq Spectra* 24(1):139–171
- Cornell CA (1968) Engineering seismic risk analysis. *Bull Seismol Soc Am* 58:1583–1606
- Engdahl ER, Jackson JA, Myers SC, Bergman EA, Priestley K (2006) Relocation and assessment of seismicity in the Iran region. *Geophys J Int* 167:761–778
- Gardner JK, Knopo L (1974) Is the sequence of earthquakes in Southern California, with aftershocks removed, Poissonian? *Bull Seismol Soc Am* 64(5):1363–1367
- Ghodrati Amiri G, Razavian Ameri SA, Motamed R, Ganjavi B (2007) Uniform hazard spectra for different northern part of Tehran, Iran. *J Appl Sci* 22:3368–3380
- Jackson JA, Priestley K, Allen M, Berberian M (2002) Active tectonics of the South Caspian Basin. *Geophys J Int* 148:214–245
- Mc Guire RK (1995) Probabilistic seismic hazard analysis and design earthquake: closing the loop. *Bull Seismol Soc Am* 85:1275–1284
- Nowroozi AA (2010) Probability of peak ground horizontal and peak ground vertical accelerations at Tehran and surrounding areas. *Pure appl Geophys* 167:1459–1474
- Ritz JF, Nazari H, Salamati HAR, Shafeii A, Solaymani S (2006) Active transtension inside Central Alborz: a new insight into the Northern Iran–Southern Caspian geodynamics. *Geology* 34:477–480
- Schwartz DP, Coppersmith KJ (1984) Fault behaviour and characteristic earthquakes: examples from the Wasatch and San Andreas Fault Zones. *J Geophys Res* 89:5681–5698
- Stapp JC (1972) Analysis of completeness of the earthquake sample in the Puget Sound area and its effects on statistical estimate of earthquake hazard. In: *Proceedings First Microzonation Conference, Seattle, USA*, pp 897–909
- Tchalenko JS (1975) Seismicity and structure of Kopet Dagh (Iran). *Phil Trans Roy Soc Lond* 278:1–25
- Vernant P, Nilforoushan F, Bayer R, Chéry J, Djamour Y, Masson F, Nankali H, Ritza J-F, Sedighi M, Tavakoli F (2004) Deciphering oblique shortening of central Alborz in Iran using geodetic data. *Earth Planet Sci Lett* 223:177–185
- Yaghmaei-Sabegh S, Lam NTK (2010) Ground motion modeling in Tehran based on the stochastic method. *Soil Dyn Earthq Eng* 30:525–535
- Yazdani A, Shahpari A, Salimi MR (2012) The use of Monte-Carlo simulations in seismic hazard analysis in Tehran and surrounding areas. *Int J Eng* 25:159–165
- Zafarani H, Noorzad A, Ansari A, Barghi K (2009) Stochastic modeling of Iranian earthquakes and estimation of ground motion for future earthquake in Greater Tehran. *Soil Dyn Earthq Eng* 29:722–741
- Zolfaghari MR (1998) GIS-based seismic hazard assessment for Iran. Ph.D. dissertation, Department of Civil Engineering, Imperial College, London, 249 pp
- Zolfaghari MR (2009) Use of raster-based data layers to model spatial variation of seismotectonic data in probabilistic seismic hazard assessment. *J Comput Geosci* 35:1460–1469